Article

Cell Reports

Frizzled-Induced Van Gogh Phosphorylation by CK1ε Promotes Asymmetric Localization of Core PCP Factors in *Drosophila*

Graphical Abstract

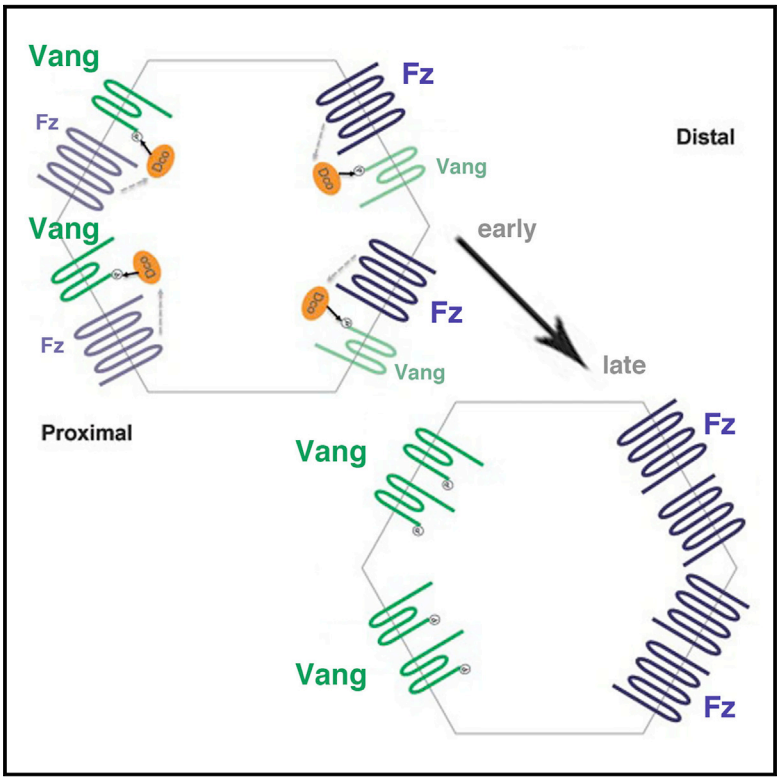

Highlights

- Fz induces Vang phosphorylation in a cell-autonomous but Dsh-independent manner
- CK1ε/Dco mediates Vang phosphorylation on conserved N-terminal serine residues
- Phosphorylation is critical for polarized localization and function of Vang in PCP

Authors

Lindsay K. Kelly, Jun Wu, Wang A. Yanfeng, Marek Mlodzik

Correspondence

marek.mlodzik@mssm.edu

In Brief

Kelly et al. find that Vang phosphorylation is involved in planar cell polarity (PCP) signaling. This phosphorylation is mediated by CK1ε/Dco and requires cell-autonomous Frizzled signaling activity but is independent of Dsh function. Vang phosphorylation is essential for polarized membrane localization and Vang function in PCP.

Kelly et al., 2016, Cell Reports *16*, 344–356
July 12, 2016
http://dx.doi.org/10.1016/j.celrep.2016.06.010

CellPress

OPEN ACCESS
CellPress

Cell Reports
Article

Frizzled-Induced Van Gogh Phosphorylation by CK1ε Promotes Asymmetric Localization of Core PCP Factors in *Drosophila*

Lindsay K. Kelly,[1] Jun Wu,[1] Wang A. Yanfeng,[1] and Marek Mlodzik[1,*]
[1]Department of Developmental & Regenerative Biology and Graduate School of Biomedical Sciences, Icahn School of Medicine at Mount Sinai, 1 Gustave L. Levy Place, New York, NY 10029, USA
*Correspondence: marek.mlodzik@mssm.edu
http://dx.doi.org/10.1016/j.celrep.2016.06.010

SUMMARY

Epithelial tissues are polarized along two axes. In addition to apical-basal polarity, they are often polarized within the plane of the epithelium, so-called Planar Cell Polarity (PCP). PCP depends upon Wnt/Frizzled (Fz) signaling factors, including Fz itself and Van Gogh (Vang/Vangl). We sought to understand how Vang interaction with other core PCP factors affects Vang function. We find that Fz induces Vang phosphorylation in a cell-autonomous manner. Vang phosphorylation occurs on conserved N-terminal serine/threonine residues, is mediated by CK1ε/Dco, and is critical for polarized membrane localization of Vang and other PCP proteins. This regulatory mechanism does not require Fz signaling through Dishevelled and thus represents a cell-autonomous upstream interaction between Fz and Vang. Furthermore, this signaling event appears to be related to Wnt5a-mediated Vangl2 phosphorylation during mouse limb patterning and may thus be a general mechanism underlying Wnt-regulated PCP establishment.

INTRODUCTION

Most epithelial tissues show cellular polarization, crucial for tissue integrity and specialized functions. Besides apical-basal polarization, epithelial cells are often organized along an orthogonal axis of polarity, referred to as planar cell polarity (PCP) (Adler, 2012; Bayly and Axelrod, 2011; Devenport, 2014; Goodrich and Strutt, 2011; Klein and Mlodzik, 2005; Seifert and Mlodzik, 2007; Wang and Nathans, 2007; Wu and Mlodzik, 2009; Zallen, 2007).

PCP establishment is mediated by conserved core components of the Wnt/Frizzled-PCP pathway. These components include the seven-pass transmembrane receptor Frizzled (Fz), the homotypic cell adhesion molecule Flamingo (Fmi; also known as Starry Night/Stan in *Drosophila*; Celsr in mammals), the four-pass transmembrane protein Van Gogh (Vang, a.k.a. Strabismus/Stbm in *Drosophila*; Vang-like/Vangl in vertebrates), and the cytoplasmic factors Dishevelled (Dsh), Diego (Dgo; Inversin/Diversin in vertebrates), and Prickle (Pk) (Adler, 2012; Bayly and Axelrod, 2011; Devenport, 2014; Goodrich and Strutt, 2011; Seifert and Mlodzik, 2007; Wu and Mlodzik, 2009; Zallen, 2007). Molecular interactions resolve these factors into two antagonistic complexes that are stably localized to opposing cell membranes. Polarized localization and/or activation of these cytoplasmic factors then directs PCP signaling to tissue-specific downstream effectors (Adler, 2012; Bayly and Axelrod, 2011; Seifert and Mlodzik, 2007; Singh and Mlodzik, 2012).

PCP has been most studied and is best understood in *Drosophila*, due to the ease of experimental accessibility and powerful genetic tools. Here, PCP is visible in all adult cuticular structures, including the wing, thorax, abdomen, and eye (Adler, 2002; Goodrich and Strutt, 2011; Lawrence et al., 2007; McNeill, 2010; Seifert and Mlodzik, 2007). In the eye, PCP regulates cell-fate determination within the R3-R4 photoreceptor pair (Mlodzik, 1999; Strutt and Strutt, 1999). Specification of this photoreceptor pair directs rotation of ommatidia, leading to a mirror image arrangement of chiral forms across the dorso-ventral midline (often called the equator). In *Drosophila* wings, arguably the tissue with the simplest PCP readout, PCP signaling positions a single-actin-based hair at the distal vertex of each cell (Goodrich and Strutt, 2011; Seifert and Mlodzik, 2007; Wong and Adler, 1993). Approximately 28–30 hr after puparium formation (APF), strong polarization of the PCP core factors is detected: Fz, Dsh, and Dgo localize to distal cell borders of wing cells, whereas Vang and Pk localize to the proximal edges; Fmi co-localizes with both distal and proximal complexes, binding individually to Fz and Vang as well as stabilizing the two complexes across cell membranes by binding homophilically (Axelrod, 2001; Bastock et al., 2003; Feiguin et al., 2001; Shimada et al., 2001; Strutt, 2001; Tree et al., 2002). The absence of Fz, Vang, or Fmi results in loss or strongly reduced apical localization of the other core components as well as loss of PCP.

PCP establishment includes at least two layers of regulation: (1) an early phase providing global orientation of cellular polarity, which is at least in part a response to the direction of Wnt gradients (Wu et al., 2013), and (2) an amplification of this initial polarization through feedback loop interactions (both intra and inter-cellular) among the core PCP proteins (Adler, 2012; Bayly and Axelrod, 2011; Seifert and Mlodzik, 2007; Singh and Mlodzik, 2012). During both phases, non-autonomous (intercellular)

interactions can lead to polarity changes of neighboring cells; clonal analyses of the core PCP factors Fz and Vang have established that polarity is not only altered within *fz* or *Vang* mutant cells, but also in surrounding wild-type tissue. Cells surrounding a *fz* mutant clone will reorient hairs to point toward the mutant tissue, while *Vang* mutant clones induce non-autonomous changes in the opposite direction (Taylor et al., 1998; Vinson and Adler, 1987; Wu and Mlodzik, 2008). Double-mutant *Vang; fz* clones behave like *fz* single-mutant clones, suggesting that Fz is important in defining the direction of non-autonomy (Wu and Mlodzik, 2008). In contrast, *fz* clones in a *Vang* mutant background fail to re-polarize surrounding tissue, which implies that Vang has a unique function in receiving and interpreting polarity information (Strutt and Strutt, 2008). Biochemical and cell-culture experiments have shown that Fz and Vang physically interact in *trans*, which requires the cysteine-rich domain of the extracellular Fz N terminus (Strutt and Strutt, 2008; Wu and Mlodzik, 2008). It has been proposed that through this interaction, Vang can act as a Fz-CRD receptor to sense Fz activity/levels in neighboring cells. This suggests that the formation of these asymmetric intracellular complexes contributes to coordination of polarity across a tissue (Lawrence et al., 2007; Wang and Nathans, 2007; Wu and Mlodzik, 2009).

Vang is a four-pass transmembrane protein with intracellular N- and C-terminal regions. It physically interacts with Pk and the apical-basal polarity determinant Scribble through regions in its C-terminal tail (Courbard et al., 2009; Montcouquiol et al., 2003; Wolff and Rubin, 1998). It can also interact with Dsh and Dgo, although these interactions are more transient and thought to be antagonistic (Bastock et al., 2003; Das et al., 2004). Its homologs (*Vangl1 and Vangl2*) regulate all PCP processes studied in vertebrates, including neural tube closure (Jessen et al., 2002; Marlow et al., 1998; Simons and Mlodzik, 2008; Wallingford, 2006; Ybot-Gonzalez et al., 2007), and lethal mutations of both *Vangl1* and *Vangl2* have been identified in patients affected with *spina bifida* and *chraniorachischisis* (Lei et al., 2010).

In order to better define the mechanisms underlying Vang regulation, we investigated how its signaling is affected by interactions with other core PCP factors. It was previously shown that a mouse Wnt5a gradient can generate graded Vangl2 phosphorylation during proximo-distal limb patterning (Gao et al., 2011). It is unclear as to whether Wnt5 provides permissive or instructive cues for regulating PCP signaling (and Vangl2 phosphorylation), and additionally how a Wnt5 signal reaches Vangl2. Because there are several vertebrate Fz family members with redundant functions, their involvement in Vang phosphorylation remains unclear.

We attempted to circumvent the above complications in vertebrates by examining this event in vivo in *Drosophila*, where there is only one PCP-dedicated Fz. Our co-transfection approach in S2 cells initially revealed that Fz induces Vang phosphorylation. We confirmed both in S2 cells and in vivo that this Vang phosphorylation is dependent on cell-autonomous Fz signaling, but independent of Dsh, and requires membrane localization of Vang. The relevant phosphorylation sites map to two conserved N-terminal serine residues, and these are required for polarized membrane localization and Vang function. Finally, through biochemical and genetic interactions, we demonstrate that Casein kinase I epsilon (CKIε, *discs overgrown/dco* in *Drosophila*) mediates this phosphorylation event to regulate Vang signaling during PCP establishment.

RESULTS

Fz Induces Phosphorylation of Vang in S2 Cells and In Vivo

At the genetic and molecular levels, Vang can interact with all other core PCP proteins (Bastock et al., 2003; Das et al., 2004; Feiguin et al., 2001; Taylor et al., 1998; Usui et al., 1999; Wolff and Rubin, 1998; Wu and Mlodzik, 2008). To better understand the functional consequences of these interactions, we examined the behavior of Vang protein in cultured S2 cells via pairwise co-transfection experiments. When transfected alone, Vang ran as a collapsed double band on a western blot (Figures 1A, S1A, and S1B, left panels). When co-transfected with Fz, the top band of the Vang doublet migrated slower and the lower band was weaker (Figures 1A, S1A, and S1B, left). Incubation of cell lysates with lambda protein phosphatase eliminated this band shift, indicating that it is due to a phosphorylation event (Figure S1C).

Next, we wished to address the Vang phosphorylation hypothesis in vivo, by evaluating larval lysates from flies expressing *tub-Vang3XFlag* (Figure 1B). Strikingly, the phosphatase treatment caused in vivo lysates of Vang to migrate faster than untreated or mock treated lysates (Figure 1B). We then asked whether the phosphorylation depends on the presence of Fz (as in S2 cells), by comparing lysates from *tub-Vang3XFlag* transgenic larvae (in an otherwise wild-type background) to those from fz^{P21} null mutant larvae (Figures 1C, S1A, and S1B, right). We observed a "shifted" band on a western blot in wild-type lysate as compared to fz^{p21} mutant lysates, indicating that Fz is required for Vang phosphorylation (Figures 1C, S1A, and S1B). In co-transfected samples we also observed increased signals with phospho-serine and phospho-threonine antibodies as compared to the minimal signals in control samples (Figure S1D). It is worth noting that the migratory behavior of Vang was slightly different between S2 cells and in vivo samples (see Figures S1A and S1B for additional discussion and full-scale blots). Taken together, these data indicate that Vang is phosphorylated both in vivo and in cell culture in a Fz-dependent manner.

Fz Induces Vang Phosphorylation in a Cell-Autonomous Manner

In vivo, PCP is specified through cell-autonomous and non-autonomous interactions among the core PCP factors. In particular, both *fz* and *Vang* mutant clones affect the polarity of genetically wild-type neighboring cells (see Introduction). The CRD (cysteine-rich domain) within the N-terminal extracellular region of Fz physically interacts with Vang across cell membranes in vivo and in cell culture (Strutt and Strutt, 2008; Wu and Mlodzik, 2008). A *fz* mutant lacking the CRD can rescue cell-autonomous PCP defects but does not rescue the non-autonomous Fz requirement (Figure 1J; Wu and Mlodzik, 2008). When tested in S2 cells for its effect on Vang phosphorylation, FzΔCRD still induced a Vang band shift indistinguishable from wild-type Fz (Figure 1D). Likewise, lysate from fz^{p21} mutant larvae expressing *tub-FzΔCRD* also showed a band shift, similar

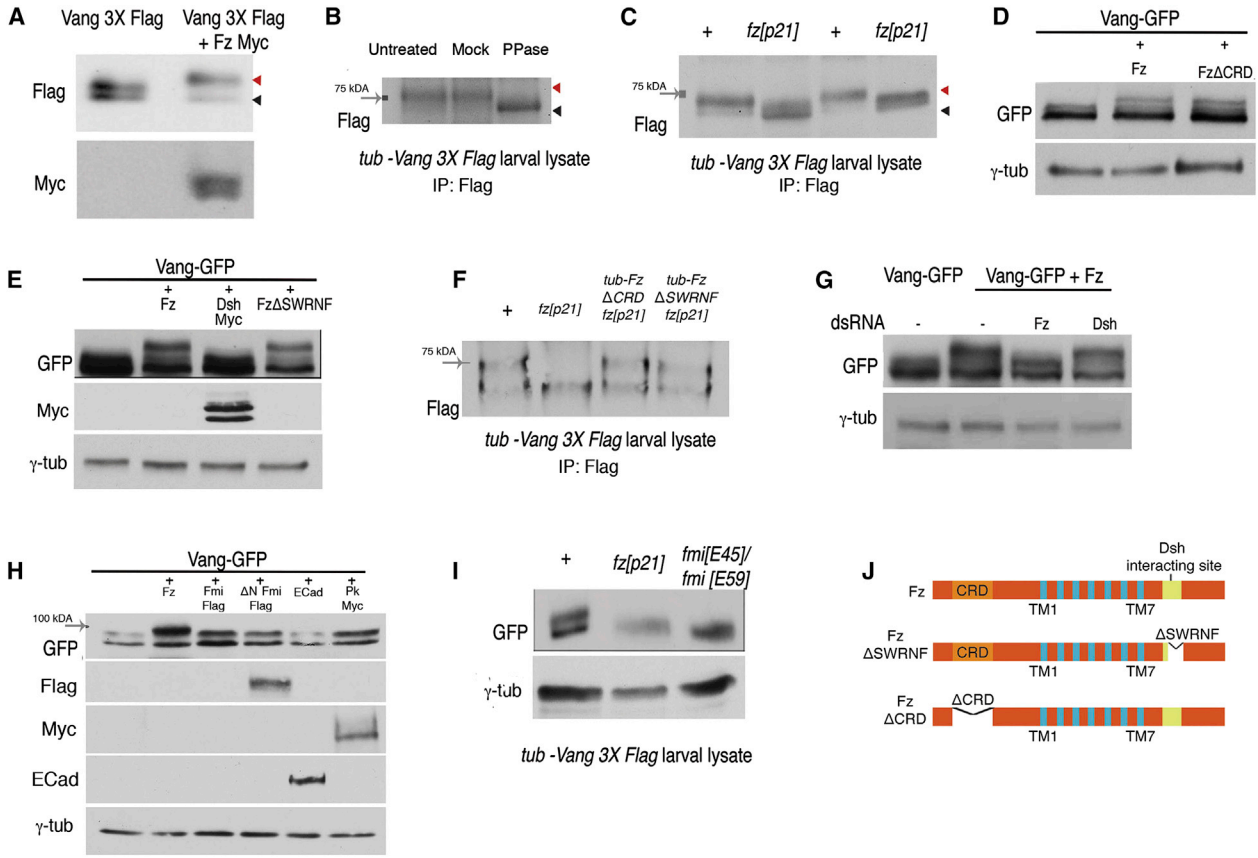

Figure 1. Fz Specifically Promotes Phosphorylation of Vang

(A–C) Vang is phosphorylated in a Fz-dependent manner. (A) Western blot analysis of Vang3XFlag and Vang3XFlag co-transfected with Fz-myc in S2 cells. Co-transfection of Fz causes a shift in the upper band of the Vang3XFlag doublet (red arrowhead; black arrowhead marks unshifted band). (B) Treatment of larval lysate with lambda protein phosphatase eliminates the Vang band shift (black arrowhead), indicating that it is caused by phosphorylation. The 75-kDa molecular weight marker is indicated by the gray arrow. (C) Western blot of in vivo lysate from *tub-Vang3XFlag* larvae in a wild-type and homozygous *fz*-null mutant background (fz^{P21}). In the absence of Fz, the Vang band shift is not observed (shifted bands are marked with red arrowhead, unshifted bands marked with black arrowhead). See Figure S1 for examples of full blots.

(D) Cell-autonomous Fz requirement for Vang phosphorylation: FzΔCRD induces a VangGFP band shift, similar to wild-type Fz in S2 cells.

(E) Cotransfection of Dsh with Vang in S2 cells does not induce a Vang-GFP band shift. FzΔSWRNF (lacking Dsh interacting site) induces a band shift, indistinguishable from WT Fz.

(F) Fz-dependent Vang phosphorylation is cell autonomous and Dsh independent in vivo. Larval lysate from fz^{p21} mutant flies expressing *tub-FzΔCRD* or *tub-FzΔSWRNF* display a band shift similar to wild-type.

(G) Knockdown of Dsh via dsRNA in S2 cells does not affect the Fz-induced Vang-GFP band shift.

(H) Cotransfection of either Fmi, ΔN-Fmi, E-Cad, or Pk with Vang in S2 cells does not induce a Vang-GFP band shift.

(I) In vivo lysates from *tub-VangGFP* expressing wing discs do not show a Vang band shift in a *fmi* mutant background (fmi^{E45}; *GAL4-1407*/fmi^{E59}; *UAS-Fmi*: Fmi was expressed from the GAL4-1407 driver to rescue embryonic and larval lethality).

(J) Schematic presentation of wild-type Fz and Fz mutant isoforms used in the above experiments. Transmembrane domains are shown in blue. FzΔSWRNF lacks the Dsh interacting site, and FzΔCRD lacks the CRD (N-terminal cysteine-rich domain) required for non-autonomous Fz signaling and function.

to lysates from wild-type larvae (Figure 1F). We therefore conclude that the CRD region of Fz is not required for regulating Vang phosphorylation, which suggests that Fz regulates phosphorylation of Vang within the same cell.

Dsh-Mediated Fz Signaling Is Not Required for Vang Phosphorylation

Dsh is a key cell-autonomous effector of Fz in the PCP pathway (Boutros and Mlodzik, 1999; Wallingford and Habas, 2005). The C-terminal cytoplasmic tail of all Fz family proteins contains a conserved motif, SWRNF (Figure 1J) that is important for the Fz-Dsh interaction. A Fz mutant lacking the SWRNF motif (FzΔSWRNF) is unable to recruit Dsh to the membrane and fails to rescue polarity defects of a fz^{-} mutant (Wu et al., 2008). Cotransfection of FzΔSWRNF and Vang in S2 cells induced phosphorylation of Vang, indistinguishable from wild-type Fz (Figure 1E). The same effect was observed in vivo, using larval lysate from fz^{p21}; *tub-FzΔSWRNF* flies (Figure 1F). Moreover, co-transfection of Dsh with Vang also failed to induce Vang phosphorylation (Figure 1E), suggesting that Dsh is not required in this process. In accordance, knockdown of Dsh by double-stranded RNA (dsRNA) in S2 cells did not affect the Fz-induced

band shift of Vang (Figure 1G; efficiency of dsRNA knockdown shown in Figure S1E). These data suggest that Fz-induced Vang phosphorylation occurs "upstream" or in parallel to Dsh function.

We hypothesized that Fz may promote Vang phosphorylation by affecting its localization to core PCP complexes. Therefore, we reasoned that Fmi might be able to provide a similar function, as it is part of the membrane localized core complexes and has been shown to promote Vang membrane association in cell culture (Shimada et al., 2001; Strutt and Strutt, 2008; Strutt et al., 2011; Usui et al., 1999). However, co-transfection of Fmi with Vang did not induce a Vang band shift in S2 cells (Figures 1H and S1F–S1G′; neither did E-cadherin or Pk, as controls). These data imply that Vang phosphorylation specifically requires Fz cell autonomously through an as yet unidentified mechanism.

Membrane Localization Is Required for Vang Phosphorylation

Importantly, when testing the genetic requirements for Vang phosphorylation in vivo, we observed a loss of the Vang band shifts in *tub-VangGFP* larval lysates not only in $fz^{-/-}$ backgrounds, but also in a *fmi* mutant background (Figure 1I). Combined with the cell-culture studies, this suggested that Fmi is necessary but not sufficient to induce Vang phosphorylation. Since proper membrane localization of both Fz and Vang in epithelial cells is (genetically) dependent on Fmi (Chen et al., 2008; Struhl et al., 2012; Strutt and Strutt, 2008, 2009), we hypothesized that a lack of Vang phosphorylation in *fmi* mutants could be related to membrane localization defects of Fz and Vang, rather than loss of Fmi "signaling" activity.

To support the notion that Vang phosphorylation depends on proper protein localization at the plasma membrane, we assessed the phosphorylation pattern of a trafficking defective Vang mutant. A "YYXXF" motif (corresponding to residues 279–283) in the Vangl2 C-terminal tail was previously shown to be a sorting signal motif, required for interaction with AP-1 subunits for export from the TGN (*trans*-Golgi network) to cell membranes (Guo et al., 2013). Substitution of VangY341 (equivalent to mouse/human Vangl2 Y279) for phenylalanine caused intracellular localization/retention of VangY341FGFP in pupal wings and failed to rescue PCP defects of *Vang* mutants (see eye and wing examples in Figures 2E–2L), whereas wild-type VangGFP (control) localized to proximal cell borders within the proximal-distal axis as expected (Figures 2A–2B″). Surprisingly, phenylalanine substitution of the neighboring tyrosine residue, Y342 (corresponding to Vangl2 Y280), had no effect on Vang localization (Figures S2A–S2B″), which contrasts with experiments in COS7 cells, where the equivalent mutant (Y280A) was transport defective (Guo et al., 2013). Consistent with this difference, VangY342F rescued the PCP defects of a *Vang*-null allele and localized to the plasma membrane like WT-VangGFP (Figure S2). In contrast, VangY341F failed to rescue PCP defects of *Vang* mutants in all tissues analyzed (eye and wing examples in Figures 2E–2L). Importantly, VangY341F-GFP did not undergo phosphorylation when cotransfected with Fz in S2 cells (Figure 2C), and in vivo larval lysates from *tub-VangY341F-GFP* (in $Vang^{-/-}$ mutant backgrounds) flies did not produce a band shift (Figure 2D). Consistent with Vang membrane localization requirements for phosphorylation and function, VangY342FGFP was phosphorylated indistinguishably from WT-VangGFP (Figure S2C). Together, these data imply that Fz-induced Vang phosphorylation occurs at the plasma membrane.

Vang Is Phosphorylated on N-Terminal Serines

Vang is a four-pass transmembrane protein with small extracellular loops. We thus reasoned that phosphorylation (as detected by the band shift) likely occurs on its intracellular regions, the N-terminal cytoplasmic tail (residues 1–149), the intracellular loop (222–235), or the C-terminal tail (303–584) (Figures 3A and S3A). Using truncated versions of Vang, we established that protein constructs containing only the C-terminal tail failed to undergo the phosphorylation-dependent band shift when co-transfected with Fz (Figure S3B). We therefore examined the intracellular N terminus, which contains a conserved cluster of serine (S) and threonine (T) residues (Figures 3A and S3A) that were also detected as phosphorylated in mouse Vangl2 (Gao et al., 2011). Point mutagenesis of S109 to Ala (S109A), S110A, and S113A in the N-terminal half of this cluster (N-term mut-3xFlag; Figure 3B) did not affect Vang phosphorylation. However, mutagenesis of the C-terminal half (C-term mut-3xFLAG) of the cluster (T116A, S117A, S120A, S122A; Figure 3B) strongly reduced Vang band shifts. Detailed mutagenesis demonstrated that S120 and S122 were essential for the phosphorylation event (Figure 3B). Single substitutions of individual S120 or S122 residues did not affect Vang band shifts (Figure S3C), indicating that both are equivalent and sufficient for the event.

We confirmed the requirement of these residues in vivo by generating transgenic flies expressing Vang with S120A/S122A substitutions (VangS2A mutant). Consistent with the S2 cell studies, larval lysate from *tub-VangS2Amut-GFP* flies did not produce a band shift (compared to control *tub-VangGFP*; Figure 3C).

Ser120/122 Phosphorylation Is Required for Vang Function

The VangS2A mutant transgene was then used to address whether the respective phosphorylation is important for Vang function in vivo. In the wing, *Vang*-null mutants have hair orientation defects and multiple cellular hairs (Vinson and Adler, 1987; Wolff and Rubin, 1998), which can be rescued by expression of *tub-VangGFP* (Figures 3D and 3E; see also Bastock et al., 2003; Strutt, 2002). Expression of *tub-VangS2A-GFP* in *Vang* mutants did not rescue the PCP defects, with many wing regions showing misoriented hairs (Figure 3F). In the eye, *Vang* mutants display classical PCP phenotypes reflected by ommatidial chirality and orientation defects. Whereas *tub-VangGFP* expression in the $Vang^{-}$ background fully restored the wild-type mirror image arrangement of ommatidia across the dorsoventral midline, *tub-VangS2A-GFP* did not rescue PCP defects, showing a phenotype similar to $Vang^{-}$ mutants (Figures 3G–3I). In a wild-type background, *tub-VangS2A-GFP* expression did not cause dominant (gain-of-function) PCP phenotypes in wings or eyes, indicating that VangS2A acts as a loss-of-function mutant (Figures S3D and S3E), and the observed defects are not due to gain-of-function or dominant-negative effects of the transgene.

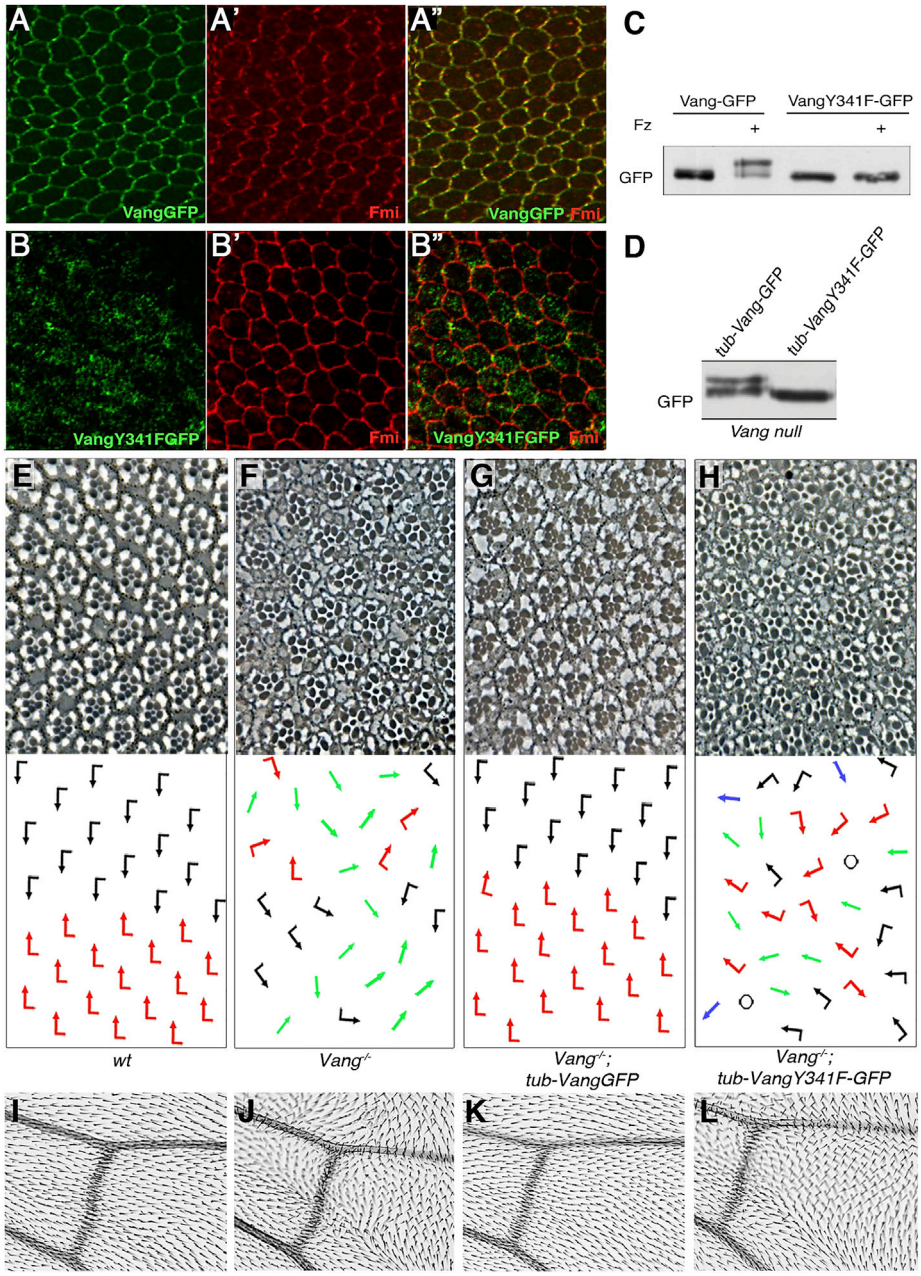

Figure 2. Membrane Localization of Vang Is Required for Vang Phosphorylation and Function in PCP

(A–B″) Pupal wings (at 30–32 hr APF), stained for GFP, detecting Vang-GFP (green), and Fmi (red). (A–A″) *tub-VangGFP* expressed in a *Vang*$^{-/-}$ background localizes like wild-type Vang to proximal membrane regions within the proximo-distal axis, overlapping with Fmi (A′ and A″). (B) *tub-Vang341F-GFP* expressed in *Vang*$^{-/-}$ mutants accumulates largely intracellularly, failing to stably localize at the membrane with Fmi (B′ and B″).

(C and D) The Vang341F-GFP mutant does not undergo the phosphorylation-induced band shift as detected in western blots, upon co-transfection with Fz in S2 cells (C), or in vivo lysates from *tub-Vang341F-GFP, Vang*$^{-/-}$ animals (D).

(E–L) VangY341F does not rescue the *Vang*$^{-/-}$ mutant phenotypes. (E–H) Tangential eye sections of indicated genotypes, showing region flanking the equator (D/V midline; anterior is left and dorsal is up); bottom panels show schematics of ommatidial orientations. Black and red arrows represent dorsal and ventral chirality; green arrows: symmetrical clusters; black dots: ommatidia with more than seven visible photoreceptors. (E) Wild-type (w^{1118}) control eye shows mirror image symmetry across the equator. (F) *Vang*$^{-/-}$ mutant exhibits chirality defects, including symmetrical ommatidia, and rotation defects. (G) Expression of *tub-VangGFP* fully rescues the *Vang*-null mutant phenotype, restoring mirror image arrangement across the equator. (H) *tub-Vang341F-GFP* fails to rescue *Vang*$^{-/-}$ polarity defects. (I–L) High magnification of adult wings, near intersection of posterior cross-vein with L4 and L5 veins; proximal is to the left, and anterior is up. (I) A single-actin-based hair extends distally from each cell in control wild-type (w^{1118}) wings. (J) *Vang*$^{-/-}$ mutants display misoriented hairs and also cells containing multiple cellular hairs. (K) *tub-VangGFP* expression fully rescues the *Vang*$^{-/-}$ PCP defects. (L) *tub-Vang341F-GFP* fails to rescue defects in *Vang*$^{-}$ wings. Scale bars represent 10 μm (E–H) and 25 μm (I–L).

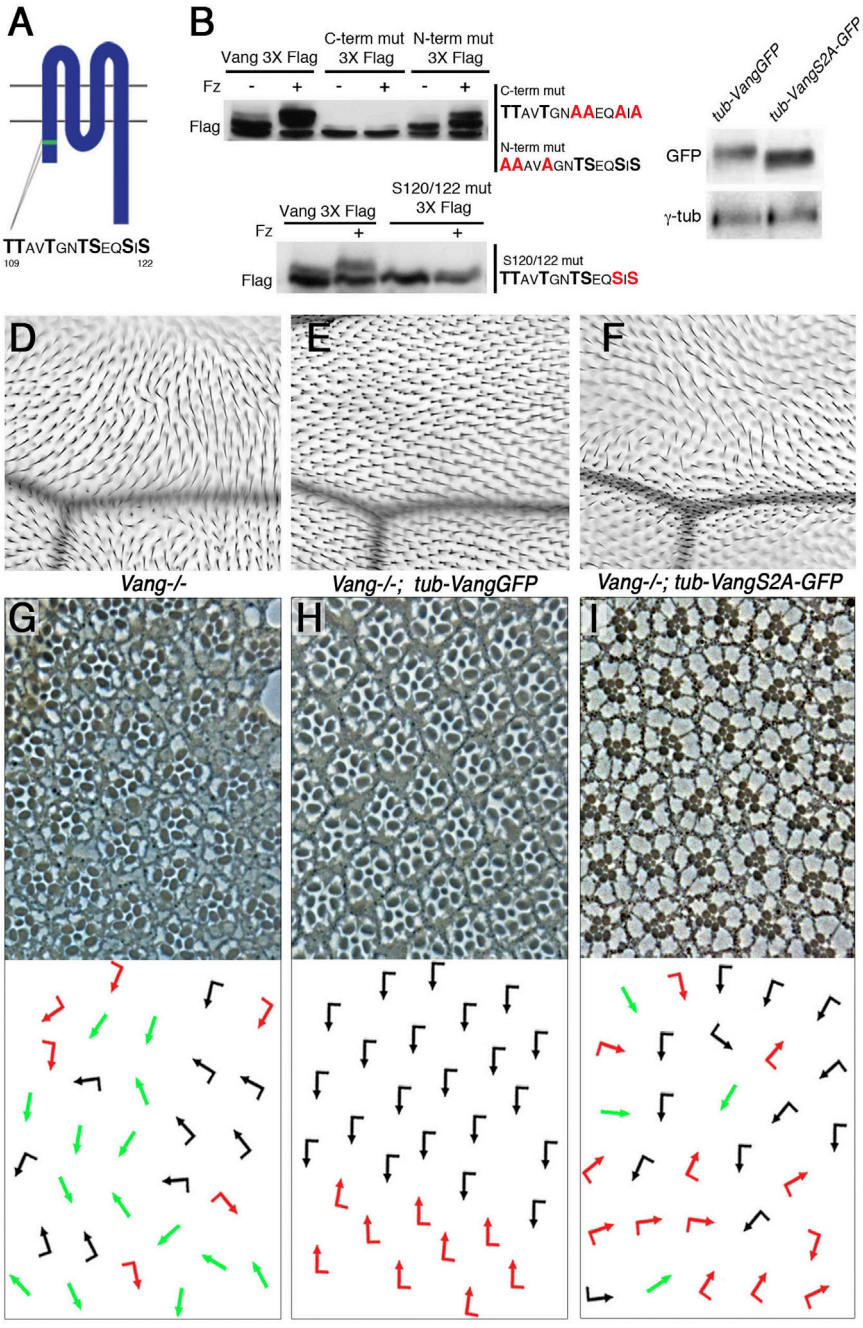

Figure 3. Vang Phosphorylation on an S/T Cluster within the Cytoplasmic N-Terminal Tail Is Required for Its Function

(A) Schematic of Vang protein structure. Green bar depicts conserved cluster of serine and threonine (S/T) residues (sequence shown below) in the intracellular N terminus.

(B) Western blot analyses of Vang3XFlag point mutants (sequence substitutions shown on right) in S2 cells. Substituting four S/T for alanine (A) in the C-terminal half of the cluster eliminates Fz-induced band shift (upper panel). Substitution of S120/122 for A is the "minimal" mutant that eliminates the Fz-induced band shift (lower panel).

(C) Larval lysate from flies expressing *tub-VangGFP* in a $Vang^{-/-}$ background displays a shifted band on a western blot, while lysates from *tub-VangS2A-GFP*; $Vang^{-/-}$ larvae did not produce a band shift.

(D–I) Vang S/T120/122 are essential for Vang function. (D–F) Adult wings (proximal is left and anterior up): region around L3 and the posterior cross vein are shown. (D) $Vang^{-/-}$ wings show hair misorientation and multiple cellular hair phenotypes. (E) Expression of *tub-VangGFP* rescues the $Vang^{-/-}$ defects, whereas *tub-VangS2A-GFP* does not rescue the $Vang^{-/-}$ defects. (G–I) Adult eye sections, near equator region of indicated genotypes. Dorsal is up and anterior is left, with schematics in bottom panels. (G) A *Vang* mutant displays chirality defects with symmetrical clusters (green arrows), as well as rotation defects. (F) *tub-VangGFP* rescues the $Vang^{-/-}$ defects. (G) Expression of *tub-VangS2A-GFP* fails to rescue the eye PCP defects of the $Vang^{-}$ mutant. Scale bars represent 25 μm (D–I).

S120/122 Phosphorylation Promotes Polarized Distribution of Vang at the Cell Membrane

Vang protein becomes polarized over time, and its asymmetric localization is indicative of functional PCP signaling (Bastock et al., 2003; Jenny et al., 2003; Strutt, 2002; Strutt and Strutt, 2009). We thus examined the localization of the VangS2A mutant compared to wild-type Vang protein in pupal wings at 32 hr APF. $Vang^{-}$ mutants rescued with wild-type *tub-VangGFP* showed strong polarization (measured by nematic order, length of white lines in Figure 4A, quantified in Figure 4G; longer lines correspond to stronger polarization) with a narrow distribution of polarity angles (Figure 4C). As among core PCP factors, there is a mutual interdependence for polarized localization, the *tub-VangGFP* rescue wings also displayed fully polarized Fmi (Figures 4A′ and A″, quantified in Figure 4H) with a narrow distribution of polarity angles (Figure 4D). In contrast, $Vang^{-}$ mutants expressing *tub-VangS2A-GFP* displayed weak, if any, Vang polarization (determined by nematic order analyses, Figures 4B and 4G), and random distribution of polarity angles within each cell (Figure 4E), with similar results observed for Fmi staining (Figures 4B′, 4F, and 4H). We conclude that this phosphorylation event is required for polarized membrane localization and/or accumulation of Vang and asymmetric core PCP localization along the proximal-distal axis.

CK1ε/Dco Binds and Phosphorylates Vang in S2 Cells

Intriguingly, several CK1 consensus sites (pS/T-X-X-S/T) exist within the S120/S122 associated S/T cluster (Figure S3A). CK1 kinases are known to affect PCP signaling through Dsh

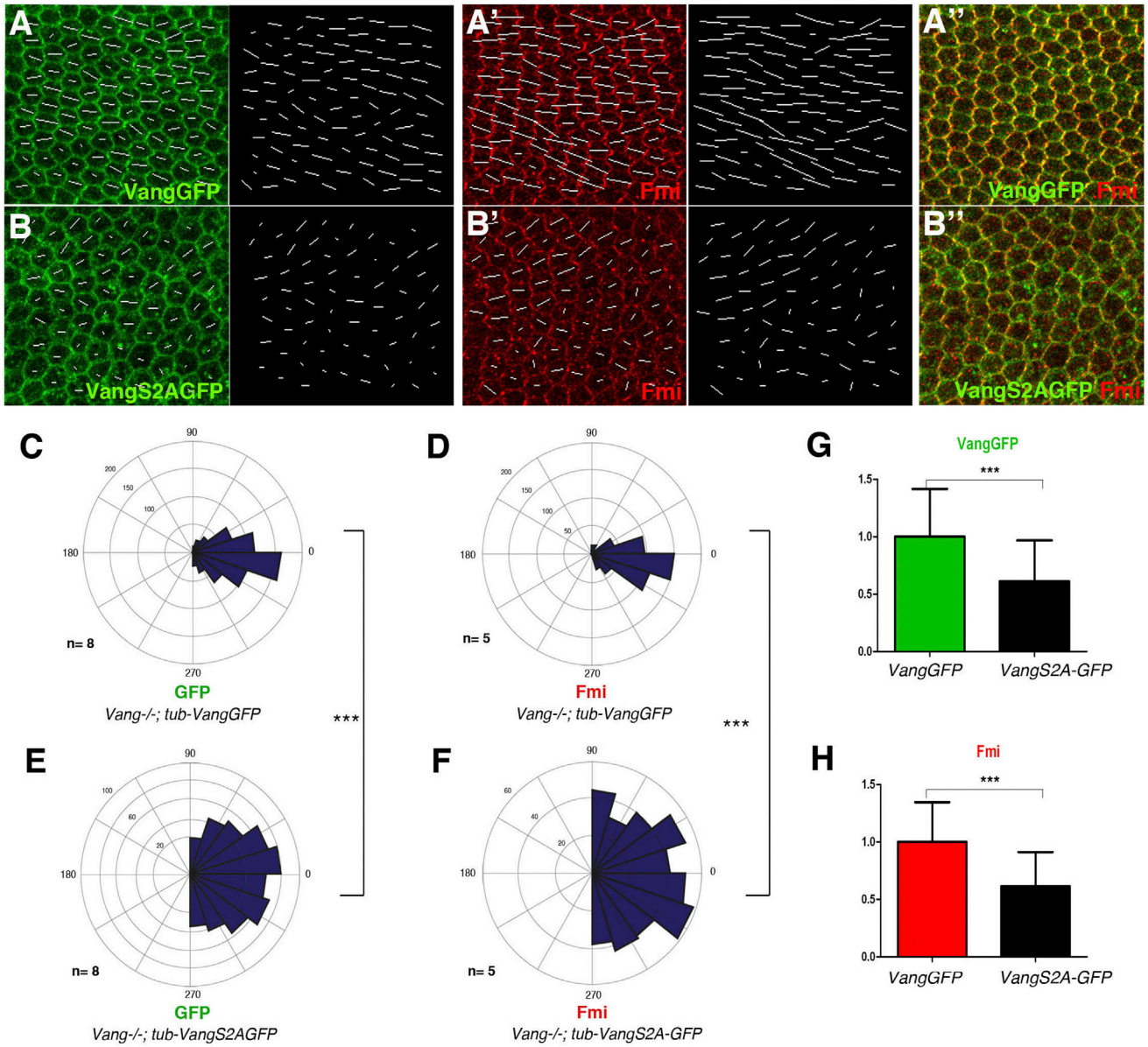

Figure 4. S120/122 Is Required for Correct Membrane Polarization or Asymmetry of Vang

(A–B″) Confocal images of 30-hr APF pupal wings stained for VangGFP (green) and Fmi (red). White lines represent nematic order, calculated by Packing Analyzer Software, with length and direction of vector lines corresponding to the magnitude and polarity axis within each cell. Scale bar. 10 μm. (A) *tub-VangGFP* (in a $Vang^{-/-}$ background) localizes to proximal membrane sides within the proximo-distal axis in pupal wing cells, co-localizing with Fmi (A′ and A″). (B) *tub-VangS2A-GFP* (in $Vang^{-/-}$) localizes to the plasma membrane uniformly, similar to Fmi in $Vang^{-/-}$ pupal wings (B′ and B″)

(C–F) Quantification of polarity angles of VangGFP (C) and Fmi (D) in $Vang^{-/-}$; *tub- VangGFP* (C and D; indistinguishable from WT) and $Vang^{-/-}$; *tub-VangS2A-GFP* (E and F). (E) PCP orientation angles of VangS2A-GFP are largely random, compared to wild-type VangGFP (C) [n = 8 for wild-type and n = 8 for VangS2A mutant; ***p < 0.001 by Student's t test of SDs for each genotype]. (F) There is also wide random range of Fmi orientation angles in $Vang^{-/-}$; *tub-VangS2A-GFP* wings (n = 5); compare to control rescue in $Vang^{-/-}$; *tub-VangGFP* wings (D) (n = 5; ***p < 0.001 by Student's t test of SDs for each genotype).

(G and H) Quantification of polarity strength (vector length) of VangGFP (G) and Fmi (H) in $Vang^{-/-}$; *tub-VangS2A-GFP* normalized to $Vang^{-/-}$; *tub-VangGFP*. (G) $Vang^{-/-}$; *tub-VangGFP* wings display, like in WT, a greater magnitude of polarization than $Vang^{-/-}$; *tub-VangS2A-GFP* wings (n = 8 for wild-type and n = 8 for VangS2A mutant, ***p < 0.01 by Student's t test). (H) Fmi polarity vectors are comparable to WT in $Vang^{-/-}$; *tub-VangGFP* wings and longer as compared to $Vang^{-/-}$; *tub-VangS2A-GFP* wings (n = 5 for wild-type and n = 5 for VangS2A mutant, ***p < 0.01 by Student's t test).

phosphorylation (Klein et al., 2006; Strutt et al., 2006), as well as regulation of vesicle trafficking (Gault et al., 2012). To test whether a *Drosophila* CK1 kinase (including CK1ε/Dco [*discs overgrown*], CK1α, and CK1γ/Gish [*gilgamesh*]) play a role in VangS120/122 phosphorylation, we co-transfected S2 cells with Vang and Fz followed by addition of a 50-μM dose of the CK1 inhibitor D4476

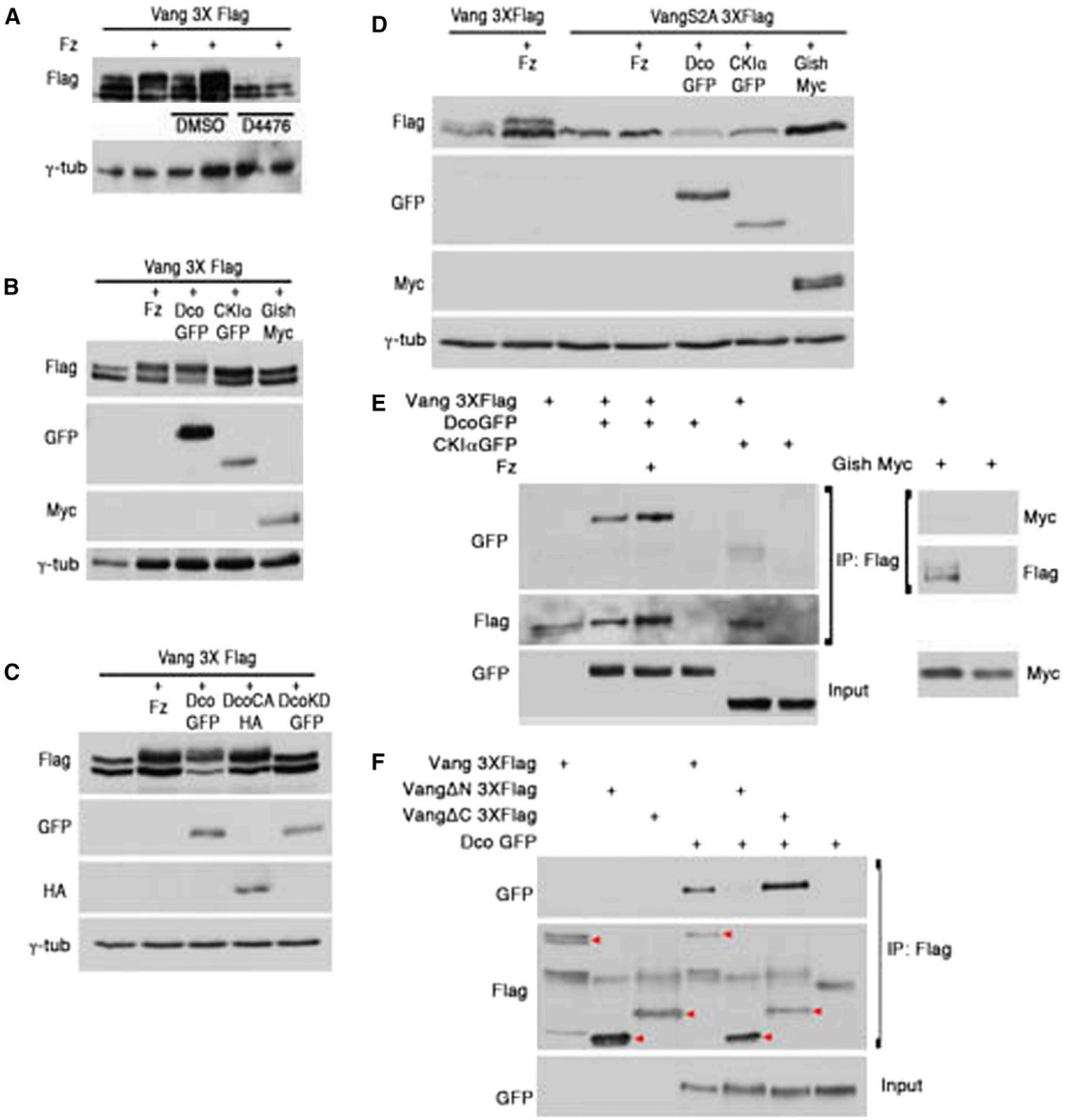

Figure 5. Vang Phosphorylation of N-Terminal S/T Cluster Is Mediated by CK1ε/Dco

(A) Lysate from S2 cells co-transfected with Vang3XFlag and Fz treated with CK1 inhibitor D4476 does not show a band shift, in contrast to DMSO-treated control cells, suggesting a CK1 family member mediates the effect.

(B) Cotransfection of Dco/CK1ε), but not other CK1 kinases (CK1α or Gish/CK1γ) induces Vang band shifts, similar to that observed with cotransfection of Fz and Vang.

(C) Constitutively active CK1ε/Dco isoform (DcoCA) induces a Vang band shift, while a kinase dead Dco mutant (DcoKD) does not.

(D) VangS2A-GFP mutant protein does not undergo a band shift when cotransfected with either Fz, CK1ε/Dco, or other CK1 kinases.

(E) Vang can co-immunoprecipitate (coIP) CK1ε/Dco (independent of Fz co-transfection). S2 cell lysates expressing Vang3XFlag and tagged CK1 proteins were immunoprecipitated with anti-Flag affinity gel and blotted with anti-GFP (upper panel) or anti-myc (lower panel). Note specific coIP of CK1ε/Dco.

(F) Vang N terminus interacts with CK1ε/Dco. DcoGFP was co-transfected with full-length Vang3XFlag, VangΔN-3XFlag or VangΔC-3XFlag, immunoprecipitated with anti-Flag and blotted with anti-GFP. Note that coIP of CK1ε/Dco with VangΔN is very weak. Red arrowheads denote Flag tagged Vang. Additional bands are due to immunoglobulin G (IgG) or non-specific background.

(Rena et al., 2004) or DMSO alone. Vang3XFlag with Fz from D4476 treated cells did not display a band shift, appearing similar to Vang3XFlag transfected alone, suggesting that a CK1 family member mediates Vang phosphorylation (Figure 5A). We next assessed which of the CK1 kinases could phosphorylate Vang in S2 cells. Upon co-transfection of Vang with each of the tagged CK1 kinases, only CK1ε/Dco was able to induce a band shift similar to that observed with co-transfection of Fz (Figure 5B).

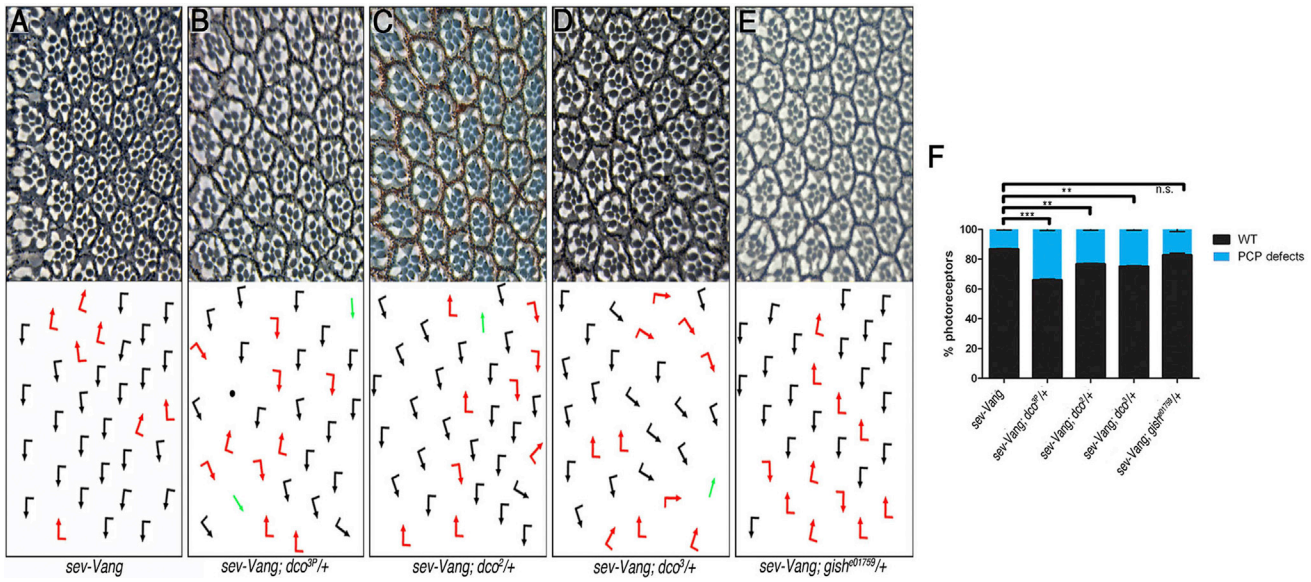

Figure 6. *Vang* and *dco* Interact Genetically In Vivo

(A–E) Eye sections near equator (see Figure 2 for WT; arrows as in Figure 2, anterior is left). Scale bar represents 15 μm. (A) *sev>Vang* expression induces mild PCP defects (rotation and chirality), which are enhanced, including symmetrical clusters and loss of photoreceptors (black dots), when one copy of *dco* is removed with the null allele (B). Less severe enhancement of PCP defects in *sev-Vang* is observed in hypomorphic $dco^{-/+}$ mutant backgrounds (C and D). Removing a copy of *gish/CK1γ* did not modify the *sev>Vang* phenotype (E).

(F) Quantification of eye phenotypes in genotypes in (A)–(E): percentage of PCP defects are shown in blue; wild-type is in black (***$p < 0.001$, **$p < 0.01$, n.s. $p > 0.05$ with Student's t test, n = 389–544 from three to four independent eyes per genotype; error bars represent SD).

Importantly, a kinase dead Dco version (Dco^{K38R}) did not induce a Vang band shift, in contrast to the a constitutively active Dco (DcoCA; Figure 5C), indicating that CK1ε kinase activity is required for this phosphorylation and suggesting that Vang is a substrate of CK1ε/Dco, as opposed to acting in a scaffolding role (Klein et al., 2006; Strutt et al., 2006). Consistent with the phosphorylation site mapping (Figures 3 and S3C), CK1ε/Dco was not able to induce phosphorylation of the VangS2A mutant isoform (Figure 5D), implying that these two serine residues are either substrates or priming sites for CK1ε/Dco (see Discussion).

Next, using co-immunoprecipitation assays in S2 cells, we asked whether Vang can form a complex with any of the CK1 family members. Consistent with the band-shift assays, we detected high levels of DcoGFP in the Vang precipitate, suggesting that Vang and Dco physically interact (Figure 5E), while only weak or minimal interactions were detected with CK1αGFP and Gish-myc, respectively (Figure 5E). To define the region of Vang binding to Dco, we tested Vang truncation constructs; VangΔN, which lacks the first 150 amino acids in the N terminus, and VangΔC, which lacks 281 amino acids comprising the intracellular C-terminal cytoplasmic tail (Figure S5B). VangΔC-3XFlag pulled down comparable amounts of DcoGFP to full-length Vang3XFlag, while VangΔN pulled down significantly less DcoGFP (Figure 5F). Though these results may be impacted by endogenous Vang protein in S2 cells, they suggested that the Vang N terminus associates with Dco. To ask whether Dco affects Vang phosphorylation in vivo, we examined larval lysates from *tub-Vang3XFlag* flies in viable hypomorphic *dco* backgrounds, given that the null allele (dco^{3P}) was lethal. In both dco^{2} and dco^{3} mutants, Vang3XFlag band shifts were not significantly affected (Figure S5A). However, as these mutants are hypomorphic alleles (and do not display PCP defects), it is likely that the remaining Dco function is sufficient to promote Vang phosphorylation, or that other CK1 kinases could act redundantly, as suggested by the physical interaction studies (see above).

dco Mutants Genetically Modify Vang Gain- and Loss-of-Function Phenotypes

Overexpression of Vang in the eye (*sev-Vang*) causes mild PCP phenotypes (approximately 15% of ommatidia display polarity defects), including chirality defects and symmetrical clusters (Figures 6A and 6F). Removing one copy of *dco* in this background, using the null allele dco^{3P}, significantly enhanced PCP defects (Figures 6B and 6F), suggesting Dco negatively regulates Vang. Correspondingly, weaker alleles (dco^{2} and dco^{3}) also enhanced *sev-Vang* though to a lesser extent (Figures 6C, 6D, and 6F). In contrast, removing one copy of *gish/CK1γ* (null allele, $gish^{e10759}$) did not modify the phenotype (Figures 6E and 6F), indicating that this interaction is specific to *dco*.

dco also genetically interacted with a *Vang* loss-of-function mutant, as PCP defects of the hypomorphic $Vang^{153}$ allele were mildly suppressed upon removing one copy of *dco* (Figures S6A–S6C). However, as *dco* also interacts with and affects Dsh function, this effect is consistent with a general PCP requirement of *dco*, and thus could be indirect.

Dco/CK1ε Regulates Vang Membrane Association and Localization

Based on the interaction data, we next investigated whether Dco affects Vang membrane accumulation/localization. We analyzed

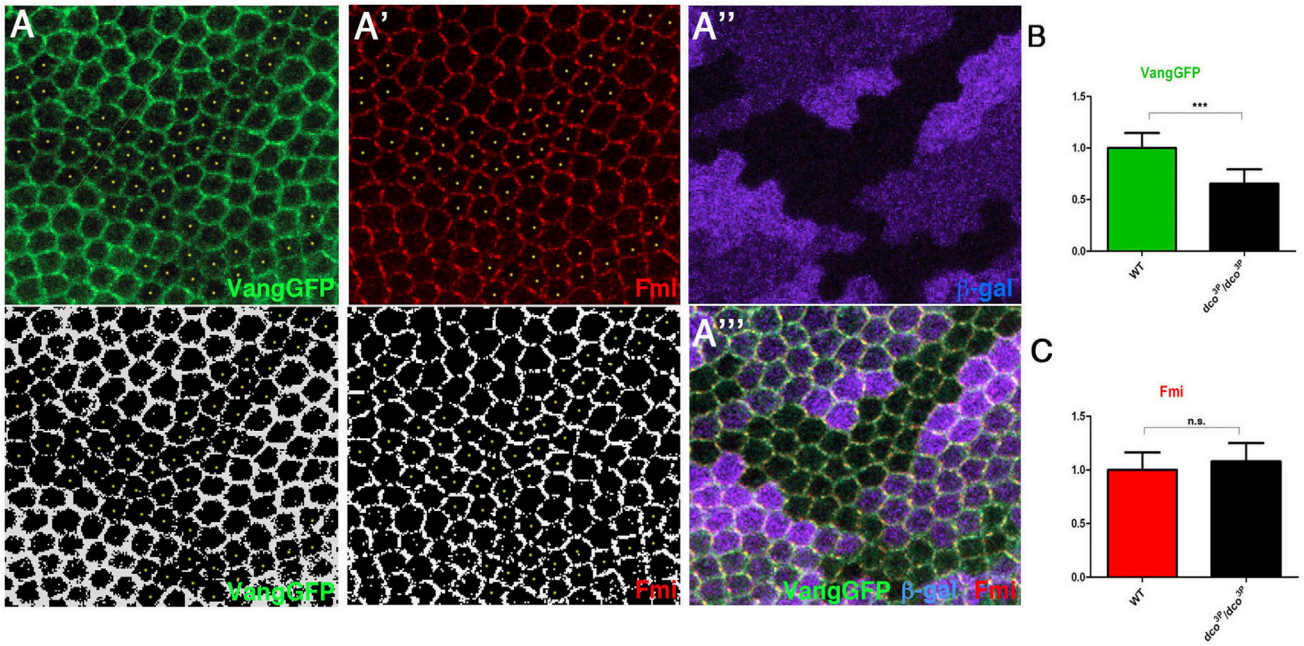

Figure 7. Vang Localization Is Affected in *dco* Mutant Clones

(A–A‴) Confocal images of immunostained pupal wings (at 30 hr APF) carrying dco^{3P} clones (marked by absence of β-Gal staining, magenta) and expressing *act-VangGFP* stained for Vang (green, monochrome in A, bottom panel) and Fmi (red, monochrome in A′, bottom panel). VangGFP levels are reduced in dco^{3P} clones (individual cells marked with yellow dots in A and A′). Scale bar represents 10 μm.

(B) Mean pixel intensity of cortical VangGFP in *dco* mutant wing tissue (n = 15), normalized to cortical VangGFP mean pixel intensity in wild-type tissue (n = 15) (***$p < 0.001$ with Student's t test, error bars represent SD).

(C) Mean pixel intensity of cortical Fmi in *dco* mutant wing tissue (n = 12 cells), normalized to cortical Fmi mean pixel intensity in wild-type tissue (n = 12 cells) (n = 5); n.s. $p > 0.05$ with Student's t test (error bars represent SD).

pupal wings at ~30–32 hr APF at the beginning of wing hair formation. At this stage, core PCP components are asymmetrically distributed at proximal-distal cell borders, and DcoGFP (*act-DcoGFP*) has been shown to localize to both proximal and distal cell edges (Strutt et al., 2006). To further study the functional relationship between Vang and Dco, we generated *dco*-null clones (dco^{3P}) and analyzed cortical VangGFP levels and distribution in mutant cells (Figure 7A; individual mutant cells not expressing β-Gal are marked with yellow dots), compared to surrounding WT tissue (Figures 7A, A″, and A‴). We observed a marked decrease of cortical VangGFP levels (VangGFP being expressed from the actin promoter that rescues the null mutant and has near-endogenous levels of Vang expression) in dco^{-} clones (Figure 7A, quantified in Figure 7B). This suggests that Dco, possibly via its kinase activity on Vang, promotes stable membrane accumulation of Vang at the proximal cell border. Although *dco* has been linked to Dsh regulation in PCP contexts (Klein et al., 2006; Strutt et al., 2006), we did not observe changes in Fmi levels inside dco^{-} cells (marked with yellow dots in Figure 7A′; compared to neighboring WT tissue and quantified in Figure 7C). This suggests that the Dco-mediated effect on Vang is rather specific.

DISCUSSION

Here, we provide evidence that serine phosphorylation within the N-terminal cytoplasmic tail of Vang is required for its polarized distribution and function in PCP signaling. We demonstrate that this phosphorylation event is dependent on Fz and occurs in a cell-autonomous manner, yet it is independent of Dsh function. We identify a CK1 family member, Dco/CK1ε, that genetically and physically interacts with Vang and mediates Vang phosphorylation in S2 cells and asymmetric Vang membrane accumulation in vivo. Biochemical experiments have identified a S/T cluster within the N-terminal cytoplasmic tail of Vang that contains CK1 consensus sequences, which are critical for Vang function. Taken together, our data suggest that Fz promotes asymmetric membrane accumulation of Vang via Dco/CK1ε-mediated phosphorylation. Strikingly, this mechanism is independent of Dsh, the cell-autonomous effector of Fz and likely acts upstream of the Dsh-Pk-Dgo-mediated cell-autonomous feedback loops. Our data thus suggest that Fz can "directly" antagonize Vang localization, rather than acting only through the cytoplasmic feedback loops. Our study provides important insight into the critical importance of the Vang N terminus and reveals an associated conserved regulatory mechanism of PCP establishment.

Fz-Induced Vang Phosphorylation Is Required for Polarized Distribution and Function of Vang in PCP

Phosphorylation of Vang on S120/122 is dependent upon Fz, in S2 cells and in vivo. Experiments with the FzΔCRD and FzΔSWRNF mutant isoforms indicate that this interaction occurs

between Fz and Vang within the same cell, but does not depend on Dsh. It is thus a cell-autonomous but Dsh-independent event and may function as an upstream antagonistic interaction between the two membrane core components.

Our data suggest that Fz-induced Vang phosphorylation serves as a mechanism to produce or reinforce asymmetric localization of PCP components. Although Fz is required for this phosphorylation to occur, its exact role remains unclear. As phosphorylation-deficient Vang (VangS2A) localizes largely uniformly at the cell cortex, a tempting hypothesis is that Fz-induced phosphorylation affects local Vang accumulation and/or stability at the distal (and lateral) cell borders, while promoting its association into stable complexes at the proximal membrane. This effect is highly specific, as Fmi also promotes Vang membrane localization but does not induce its phosphorylation. Thus Fz plays an active role in Vang phosphorylation, perhaps through regulation of kinase function or kinase recruitment to the PCP core complex. In line with this, it has been shown that CK1ε requires an activating dephosphorylation event (Rivers et al., 1998), which can be induced by Fz signaling (Swiatek et al., 2004). Conversely, it is possible that Fz may function downstream of Dco/CK1ε to prevent dephosphorylation of Vang.

Dco/CK1ε Causes Phosphorylation of the Vang Intracellular N Terminus

We show that Vang is phosphorylated on two conserved serine residues, S120 and S122, which are also phosphorylated in mouse Vangl2. Gao et al. (2011) demonstrated that these residues can act as "founder sites" for phosphorylation of additional S/T residues in the conserved cluster (Gao et al., 2011). It is likely that additional phosphorylation events are conserved from *Drosophila* to vertebrates as our work suggests. In mouse limbs, this Vangl2 phosphorylation event is dependent on Wnt5a and Ror2, but, due to the redundancy of Fz genes in the mouse, the requirement of Fzs was not addressed (Gao et al., 2011). Our data provide evidence that this mechanism is a conserved general process in PCP contexts and suggest an instructive link between the Wg/Wnt-Fz interaction in *Drosophila* (Wu et al., 2013) and Wnt5a in mouse limbs (Gao et al., 2011) to specific Vang/Vangl phosphorylation, which mediates polarized, asymmetric Vang/Vangl2 localization.

Although CK1 kinases often require a priming phosphorylation event and might not act directly on S120/122 (a possible target of a yet unknown priming kinase), these residues are absolutely essential for asymmetric Vang localization, indicating that phosphorylation in this cluster is essential in vivo. Using gel-shift assays as a readout of Vang phosphorylation, we have not been able to discern a priming event required for Vang S120/122 phosphorylation, and mutations of the other S and T residues in the cluster did not have an effect. There are several important CK1 targets (e.g., NF-AT and β-catenin) that do not require priming (Amit et al., 2002; Liu et al., 2002; Zhu et al., 1998), and thus direct CK1ε phosphorylation of these sites is plausible. Similarly, it is conceivable that S120/122 phosphorylation itself represents a priming event for additional phosphorylations within the conserved cluster.

We show that Dco binds the intracellular N terminus of Vang. The intracellular Vang C-terminal sequences are known to mediate homodimerization of Vang (Belotti et al., 2012) and binding to Pk, Dsh, Dgo, and Scrib (Bastock et al., 2003; Courbard et al., 2009; Das et al., 2004; Feiguin et al., 2001; Jenny et al., 2003, 2005); therefore, these interactions should not be directly affected by loss of Vang phosphorylation on S120/122 (VangS2A). Dco was previously shown to generally localize to the cell cortex in pupal wing cells (Strutt et al., 2006), although it is likely that its activity is differentially regulated on each side of the cell. Klein et al. (2006) demonstrated that Dco promotes Dsh phosphorylation in a kinase-activity-independent, indirect mechanism. In contrast, our data suggest that Dco acts directly on Vang as a substrate. However, as Strutt et al. (2006) also showed a reduction in Dsh levels and polarization in *dco* clones, and because there is a mutual dependence among the core PCP factors for their localization, it is impossible to determine in vivo which of these represent direct effects.

Given that CK1 family members have many defined and distinct roles in both Wnt signaling branches, the canonical Wnt pathway and Wnt-PCP signaling, it is worth considering the evolution of CK1s in these contexts. It is possible that CK1 kinases were first linked to canonical Wnt signaling and then adopted by the core PCP factors, or they may be generally associated with Fz-mediated processes and their functions evolved with the added complexity of additional Fz-mediated signaling features. It should be interesting to address such questions in primitive organisms, like hydra, that require Wnt signaling (Hensel et al., 2014; Holstein, 2008; Lengfeld et al., 2009; Philipp et al., 2009) but have fewer isoforms of the respective genes.

EXPERIMENTAL PROCEDURES

Fly Strains, Genetics, and Plasmids

Flies were raised on standard medium, maintained at 25°C, unless otherwise indicated. The following lines were used to induce dco^{dbt3P} clones: *y*, *w*, *hsFlp*; *armlacZ*, *FRT82*. Clones were induced during second and third-instar stages.

To generate *tub-Vang3XFlag* and *tub-Vang-GFP* transgenic flies, respective tags were added to the C-term of Vang by PCR amplification and cloned into pCasper-tub vectors. Various point mutants were created by Agilent QuikChange II XL site-directed mutagenesis kit. Primer sequences are available upon request. To generate tub^{-} CK1α-GFP construct, GFP was added to the C-term of CK1α sequence by PCR amplification using DGRC LD05574 cDNA clone. tub-DcoCA-HA construct: an HA tag was added after the 296 amino acids of *dco* by PCR.

Gel-Shift and Protein Binding Assays

Effectene (QIAGEN) was used to transfect DNA plasmids into S2 cells following general protocols. Cells were lysed ~48 hr after transfection in lysis buffer containing 20 mM HEPES, 100 mM NaCl, 1 mM EDTA, 1% NP-40, 10% glycerol, Sigma phosphatase inhibitor cocktail 2 and 3 (1:100) and Calbiochem protease inhibitor (1:100). Larval lysates were prepared by dissection in PBS to isolate eye/leg/wing disc complexes, followed by lysis in the buffer described above.

Samples were run on 12% Anderson gels at 70 V to achieve best separation between phosphorylated and unphosphorylated isoforms. Gels were transferred to nitrocellulose membrane and probed with appropriate antibodies.

Immunoprecipitation and coIP experiments were performed by incubating precleared lysates with anti-Flag M2 affinity gel (Sigma) at 4°C overnight followed by five washes in PBS + 0.1% Tween 20 and elution by boiling in Laemmli sample buffer.

dsRNA Knockdown and D4476 Treatment in S2 Cell Culture

dsRNA sequences for Fz and Dsh were designed using GenomeRNAi and generated using the Drosophila RNAi Screening Center at Harvard Med

School (DRSC; http://www.flyrnai.org/DRSC-PRS.html) synthesis protocols. RNAi knockdown was performed via DRSC cell bathing, followed by transfection using Effectene (QIAGEN) general protocol ~48 hr later. Cells were treated with 50 μM D4476 in DMSO (Sigma) 3 and 18 hr following transfection.

Immunohistochemistry and Immunocytochemistry

Primary antibodies were mouse anti-Flag (1:1,000, Sigma-Aldrich); mouse anti-GFP (1:1,000, Roche); rabbit anti-GFP (1:1,000, Invitrogen); rabbit anti-myc (1:1,000, Santa Cruz Biotechnology), rat anti-HA (1:500, Roche); mouse anti-Fmi (1:10, Developmental Studies Hybridoma Bank [DSHB]); and mouse anti-β-gal (1:200, DSHB). Fluorescent and horseradish peroxidase (HRP) secondary antibodies were from Jackson ImmunoResearch Laboratories.

Pupal wings were dissected and fixed in 4% formaldehyde 0.1% Triton X-100 PBS for 1–3 hr. Tissues were washed two times in 0.1% Triton X-100 PBS (PBT) and incubated in 0.1% BSA PBT for 15–30 min. Primary antibodies were added and incubated overnight at room temperature. Samples were washed three times in PBT and once in 0.1% BSA PBT. Fluorescent secondary antibodies were in 0.1% BSA PBT and incubated for 2 hr. Samples were washed four times in PBT, rinsed once in PBS, and mounted to slides in 80% glycerol 0.4% n-propyl gallate mounting media.

Wings of adult flies were collected and soaked in PBS with 0.1% Triton X-100 and carefully mounted in 80% glycerol PBS solution. Eye sections were prepared as described (Gaengel and Mlodzik, 2008). For rescue experiments and genetic interactions, eyes were sectioned near the equatorial region.

Quantitative Analysis of Pupal Wing Images and Generation of Polarity Vectors

Polarity of pupal wing stains was calculated with the software "packing_analyzer_V2" as described in (Aigouy et al., 2010). The software calculated both axis and strength of polarization (nematic order). Both measurements are based on the staining intensity around the cell cortex. Detailed methods and mathematical formulae are described in Aigouy et al. (2010). The resulting polarity "vectors" were processed via GraphPad Prism to compare length of polarity vectors and MATLAB software for "rosette"-diagram presentations and statistical analyses.

Quantitative Analysis of Cortical Vang-GFP and Fmi Levels in dco Mutant Clones

Levels of cortical Vang-GFP and Fmi were determined via ImageJ to measure mean pixel intensity of each signal around the entire cortex of cells fully contained within the clone that do not share cell borders. These data were normalized to equivalent measurements taken from wild-type cells located outside clones that do not share cell borders.

SUPPLEMENTAL INFORMATION

Supplemental Information includes six figures and can be found with this article online at http://dx.doi.org/10.1016/j.celrep.2016.06.010.

AUTHOR CONTRIBUTIONS

L.K.K. conceived the project, designed and performed experiments, analyzed data, and wrote the manuscript. J.W. performed experiments and analyzed data. W.A.Y. designed and performed initial experiments. M.M. conceived the project, designed experiments, analyzed data, and wrote the manuscript.

ACKNOWLEDGMENTS

We would like to thank the Bloomington Stock Center and DSHB for flies and antibodies, and members of M.M.'s lab for many helpful suggestions, comments, and discussions during the development and execution of the project. We are grateful to Giovanna Collu, Ashley Humphries, Robert Krauss, and Cathie Pfleger for helpful comments on the manuscript. Confocal microscopy was performed at the ISMMS Tisch Cancer Institute Microscopy Core, in part supported by grant P30 CA196521 from the NCI. This work was supported by NIGMS and NEI grants from the NIH to M.M.

Received: December 1, 2015
Revised: April 5, 2016
Accepted: May 26, 2016
Published: June 23, 2016

REFERENCES

Adler, P.N. (2002). Planar signaling and morphogenesis in Drosophila. Dev. Cell *2*, 525–535.

Adler, P.N. (2012). The frizzled/stan pathway and planar cell polarity in the Drosophila wing. Curr. Top. Dev. Biol. *101*, 1–31.

Aigouy, B., Farhadifar, R., Staple, D.B., Sagner, A., Röper, J.C., Jülicher, F., and Eaton, S. (2010). Cell flow reorients the axis of planar polarity in the wing epithelium of Drosophila. Cell *142*, 773–786.

Amit, S., Hatzubai, A., Birman, Y., Andersen, J.S., Ben-Shushan, E., Mann, M., Ben-Neriah, Y., and Alkalay, I. (2002). Axin-mediated CKI phosphorylation of beta-catenin at Ser 45: a molecular switch for the Wnt pathway. Genes Dev. *16*, 1066–1076.

Axelrod, J.D. (2001). Unipolar membrane association of Dishevelled mediates Frizzled planar cell polarity signaling. Genes Dev. *15*, 1182–1187.

Bastock, R., Strutt, H., and Strutt, D. (2003). Strabismus is asymmetrically localised and binds to Prickle and Dishevelled during Drosophila planar polarity patterning. Development *130*, 3007–3014.

Bayly, R., and Axelrod, J.D. (2011). Pointing in the right direction: new developments in the field of planar cell polarity. Nat. Rev. Genet. *12*, 385–391.

Belotti, E., Puvirajesinghe, T.M., Audebert, S., Baudelet, E., Camoin, L., Pierres, M., Lasvaux, L., Ferracci, G., Montcouquiol, M., and Borg, J.P. (2012). Molecular characterisation of endogenous Vangl2/Vangl1 heteromeric protein complexes. PLoS ONE *7*, e46213.

Boutros, M., and Mlodzik, M. (1999). Dishevelled: at the crossroads of divergent intracellular signaling pathways. Mech. Dev. *83*, 27–37.

Chen, W.S., Antic, D., Matis, M., Logan, C.Y., Povelones, M., Anderson, G.A., Nusse, R., and Axelrod, J.D. (2008). Asymmetric homotypic interactions of the atypical cadherin flamingo mediate intercellular polarity signaling. Cell *133*, 1093–1105.

Courbard, J.R., Djiane, A., Wu, J., and Mlodzik, M. (2009). The apical/basal-polarity determinant Scribble cooperates with the PCP core factor Stbm/Vang and functions as one of its effectors. Dev. Biol. *333*, 67–77.

Das, G., Jenny, A., Klein, T.J., Eaton, S., and Mlodzik, M. (2004). Diego interacts with Prickle and Strabismus/Van Gogh to localize planar cell polarity complexes. Development *131*, 4467–4476.

Devenport, D. (2014). The cell biology of planar cell polarity. J. Cell Biol. *207*, 171–179.

Feiguin, F., Hannus, M., Mlodzik, M., and Eaton, S. (2001). The ankyrin repeat protein Diego mediates Frizzled-dependent planar polarization. Dev. Cell *1*, 93–101.

Gaengel, K., and Mlodzik, M. (2008). Microscopic analysis of the adult Drosophila retina using semithin plastic sections. Methods Mol. Biol. *420*, 277–287.

Gao, B., Song, H., Bishop, K., Elliot, G., Garrett, L., English, M.A., Andre, P., Robinson, J., Sood, R., Minami, Y., et al. (2011). Wnt signaling gradients establish planar cell polarity by inducing Vangl2 phosphorylation through Ror2. Dev. Cell *20*, 163–176.

Gault, W.J., Olguin, P., Weber, U., and Mlodzik, M. (2012). Drosophila CK1-γ, gilgamesh, controls PCP-mediated morphogenesis through regulation of vesicle trafficking. J. Cell Biol. *196*, 605–621.

Goodrich, L.V., and Strutt, D. (2011). Principles of planar polarity in animal development. Development *138*, 1877–1892.

Guo, Y., Zanetti, G., and Schekman, R. (2013). A novel GTP-binding protein-adaptor protein complex responsible for export of Vangl2 from the trans Golgi network. eLife *2*, e00160.

Hensel, K., Lotan, T., Sanders, S.M., Cartwright, P., and Frank, U. (2014). Lineage-specific evolution of cnidarian Wnt ligands. Evol. Dev. *16*, 259–269.

Holstein, T.W. (2008). Wnt signaling in cnidarians. Methods Mol. Biol. *469*, 47–54.

Jenny, A., Darken, R.S., Wilson, P.A., and Mlodzik, M. (2003). Prickle and Strabismus form a functional complex to generate a correct axis during planar cell polarity signaling. EMBO J. *22*, 4409–4420.

Jenny, A., Reynolds-Kenneally, J., Das, G., Burnett, M., and Mlodzik, M. (2005). Diego and Prickle regulate Frizzled planar cell polarity signalling by competing for Dishevelled binding. Nat. Cell Biol. *7*, 691–697.

Jessen, J.R., Topczewski, J., Bingham, S., Sepich, D.S., Marlow, F., Chandrasekhar, A., and Solnica-Krezel, L. (2002). Zebrafish trilobite identifies new roles for Strabismus in gastrulation and neuronal movements. Nat. Cell Biol. *4*, 610–615.

Klein, T.J., and Mlodzik, M. (2005). Planar cell polarization: an emerging model points in the right direction. Annu. Rev. Cell Dev. Biol. *21*, 155–176.

Klein, T.J., Jenny, A., Djiane, A., and Mlodzik, M. (2006). CKIepsilon/discs overgrown promotes both Wnt-Fz/beta-catenin and Fz/PCP signaling in Drosophila. Curr. Biol. *16*, 1337–1343.

Lawrence, P.A., Struhl, G., and Casal, J. (2007). Planar cell polarity: one or two pathways? Nat. Rev. Genet. *8*, 555–563.

Lei, Y.P., Zhang, T., Li, H., Wu, B.L., Jin, L., and Wang, H.Y. (2010). VANGL2 mutations in human cranial neural-tube defects. N. Engl. J. Med. *362*, 2232–2235.

Lengfeld, T., Watanabe, H., Simakov, O., Lindgens, D., Gee, L., Law, L., Schmidt, H.A., Ozbek, S., Bode, H., and Holstein, T.W. (2009). Multiple Wnts are involved in Hydra organizer formation and regeneration. Dev. Biol. *330*, 186–199.

Liu, C., Li, Y., Semenov, M., Han, C., Baeg, G.H., Tan, Y., Zhang, Z., Lin, X., and He, X. (2002). Control of beta-catenin phosphorylation/degradation by a dual-kinase mechanism. Cell *108*, 837–847.

Marlow, F., Zwartkruis, F., Malicki, J., Neuhauss, S.C.F., Abbas, L., Weaver, M., Driever, W., and Solnica-Krezel, L. (1998). Functional interactions of genes mediating convergent extension, knypek and trilobite, during the partitioning of the eye primordium in zebrafish. Dev. Biol. *203*, 382–399.

McNeill, H. (2010). Planar cell polarity: keeping hairs straight is not so simple. Cold Spring Harb. Perspect. Biol. *2*, a003376.

Mlodzik, M. (1999). Planar polarity in the Drosophila eye: a multifaceted view of signaling specificity and cross-talk. EMBO J. *18*, 6873–6879.

Montcouquiol, M., Rachel, R.A., Lanford, P.J., Copeland, N.G., Jenkins, N.A., and Kelley, M.W. (2003). Identification of Vangl2 and Scrb1 as planar polarity genes in mammals. Nature *423*, 173–177.

Philipp, I., Aufschnaiter, R., Ozbek, S., Pontasch, S., Jenewein, M., Watanabe, H., Rentzsch, F., Holstein, T.W., and Hobmayer, B. (2009). Wnt/beta-catenin and noncanonical Wnt signaling interact in tissue evagination in the simple eumetazoan Hydra. Proc. Natl. Acad. Sci. USA *106*, 4290–4295.

Rena, G., Bain, J., Elliott, M., and Cohen, P. (2004). D4476, a cell-permeant inhibitor of CK1, suppresses the site-specific phosphorylation and nuclear exclusion of FOXO1a. EMBO Rep. *5*, 60–65.

Rivers, A., Gietzen, K.F., Vielhaber, E., and Virshup, D.M. (1998). Regulation of casein kinase I epsilon and casein kinase I delta by an in vivo futile phosphorylation cycle. J. Biol. Chem. *273*, 15980–15984.

Seifert, J.R.K., and Mlodzik, M. (2007). Frizzled/PCP signalling: a conserved mechanism regulating cell polarity and directed motility. Nat. Rev. Genet. *8*, 126–138.

Shimada, Y., Usui, T., Yanagawa, S., Takeichi, M., and Uemura, T. (2001). Asymmetric colocalization of Flamingo, a seven-pass transmembrane cadherin, and Dishevelled in planar cell polarization. Curr. Biol. *11*, 859–863.

Simons, M., and Mlodzik, M. (2008). Planar cell polarity signaling: from fly development to human disease. Annu. Rev. Genet. *42*, 517–540.

Singh, J., and Mlodzik, M. (2012). Planar cell polarity signaling: coordination of cellular orientation across tissues. Wiley Interdiscip. Rev. Dev. Biol. *1*, 479–499.

Struhl, G., Casal, J., and Lawrence, P.A. (2012). Dissecting the molecular bridges that mediate the function of Frizzled in planar cell polarity. Development *139*, 3665–3674.

Strutt, D.I. (2001). Asymmetric localization of frizzled and the establishment of cell polarity in the Drosophila wing. Mol. Cell *7*, 367–375.

Strutt, D.I. (2002). The asymmetric subcellular localisation of components of the planar polarity pathway. Semin. Cell Dev. Biol. *13*, 225–231.

Strutt, H., and Strutt, D. (1999). Polarity determination in the Drosophila eye. Curr. Opin. Genet. Dev. *9*, 442–446.

Strutt, H., and Strutt, D. (2008). Differential stability of flamingo protein complexes underlies the establishment of planar polarity. Curr. Biol. *18*, 1555–1564.

Strutt, H., and Strutt, D. (2009). Asymmetric localisation of planar polarity proteins: Mechanisms and consequences. Semin. Cell Dev. Biol. *20*, 957–963.

Strutt, H., Price, M.A., and Strutt, D. (2006). Planar polarity is positively regulated by casein kinase Iepsilon in Drosophila. Curr. Biol. *16*, 1329–1336.

Strutt, H., Warrington, S.J., and Strutt, D. (2011). Dynamics of core planar polarity protein turnover and stable assembly into discrete membrane subdomains. Dev. Cell *20*, 511–525.

Swiatek, W., Tsai, I.C., Klimowski, L., Pepler, A., Barnette, J., Yost, H.J., and Virshup, D.M. (2004). Regulation of casein kinase I epsilon activity by Wnt signaling. J. Biol. Chem. *279*, 13011–13017.

Taylor, J., Abramova, N., Charlton, J., and Adler, P.N. (1998). Van Gogh: a new Drosophila tissue polarity gene. Genetics *150*, 199–210.

Tree, D.R.P., Shulman, J.M., Rousset, R., Scott, M.P., Gubb, D., and Axelrod, J.D. (2002). Prickle mediates feedback amplification to generate asymmetric planar cell polarity signaling. Cell *109*, 371–381.

Usui, T., Shima, Y., Shimada, Y., Hirano, S., Burgess, R.W., Schwarz, T.L., Takeichi, M., and Uemura, T. (1999). Flamingo, a seven-pass transmembrane cadherin, regulates planar cell polarity under the control of Frizzled. Cell *98*, 585–595.

Vinson, C.R., and Adler, P.N. (1987). Directional non-cell autonomy and the transmission of polarity information by the frizzled gene of Drosophila. Nature *329*, 549–551.

Wallingford, J.B. (2006). Planar cell polarity, ciliogenesis and neural tube defects. Hum. Mol. Genet. *15*, R227–R234.

Wallingford, J.B., and Habas, R. (2005). The developmental biology of Dishevelled: an enigmatic protein governing cell fate and cell polarity. Development *132*, 4421–4436.

Wang, Y., and Nathans, J. (2007). Tissue/planar cell polarity in vertebrates: new insights and new questions. Development *134*, 647–658.

Wolff, T., and Rubin, G.M. (1998). Strabismus, a novel gene that regulates tissue polarity and cell fate decisions in Drosophila. Development *125*, 1149–1159.

Wong, L.L., and Adler, P.N. (1993). Tissue polarity genes of Drosophila regulate the subcellular location for prehair initiation in pupal wing cells. J. Cell Biol. *123*, 209–221.

Wu, J., and Mlodzik, M. (2008). The frizzled extracellular domain is a ligand for Van Gogh/Stbm during nonautonomous planar cell polarity signaling. Dev. Cell *15*, 462–469.

Wu, J., and Mlodzik, M. (2009). A quest for the mechanism regulating global planar cell polarity of tissues. Trends Cell Biol. *19*, 295–305.

Wu, J., Jenny, A., Mirkovic, I., and Mlodzik, M. (2008). Frizzled-Dishevelled signaling specificity outcome can be modulated by Diego in Drosophila. Mech. Dev. *125*, 30–42.

Wu, J., Roman, A.C., Carvajal-Gonzalez, J.M., and Mlodzik, M. (2013). Wg and Wnt4 provide long-range directional input to planar cell polarity orientation in Drosophila. Nat. Cell Biol. *15*, 1045–1055.

Ybot-Gonzalez, P., Savery, D., Gerrelli, D., Signore, M., Mitchell, C.E., Faux, C.H., Greene, N.D.E., and Copp, A.J. (2007). Convergent extension, planar-cell-polarity signalling and initiation of mouse neural tube closure. Development *134*, 789–799.

Zallen, J.A. (2007). Planar polarity and tissue morphogenesis. Cell *129*, 1051–1063.

Zhu, J., Shibasaki, F., Price, R., Guillemot, J.C., Yano, T., Dötsch, V., Wagner, G., Ferrara, P., and McKeon, F. (1998). Intramolecular masking of nuclear import signal on NF-AT4 by casein kinase I and MEKK1. Cell *93*, 851–861.